Dental Materials Journal 23(3) : 353−360, 2004

Morphological and Chemical Characterizations of the Interface of a Hydroxyapatite-coated Implant

Kiichirou MIMURA[1], Kouichi WATANABE[2], Seigo OKAWA[2], Masayoshi KOBAYASHI[3] and Osamu MIYAKAWA[2]

[1]Mimura Dental Clinic, Gezyo 71-5, Fujinomiya, Shizuoka 418-0114, Japan
[2]Division of Dental Biomaterial Science, Niigata University Graduate School of Medical and Dental Sciences, Gakkoucho-dori 2-5274, Niigata 951-8514, Japan
[3]EMX Laboratory, Center for Instrumental Analysis, Niigata University, Gakkoucho-dori 2-5274, Niigata 951-8514, Japan
Corresponding author, E-mail: watakou@dent.niigata-u.ac.jp

Received February 2, 2004/Accepted June 22, 2004

The present study aimed at morphological and chemical characterization of the coating-substrate interface of a commercially available dental implant coated with plasma-sprayed hydroxyapatite (HA). For this purpose, elements in the chemically and mechanically exposed substrate surfaces were analyzed by EPMA and XPS.

A thin titanium oxide film containing Ca and P was found at the interface. When the implant was subjected to mechanical stress, a mixed mode of cohesive and interfacial fractures occurred. The cohesive fracture was due to separation of the oxide film from the substrate, while the interfacial fracture was due to exfoliation of the coating from the oxide film bonded to the substrate. Analysis showed diffusion of Ca into the metal substrate, hence indicating the presence of chemical bond at the interface. However, mechanical interlocking seemed to play the major role in the interfacial bond.

Key words: Hydroxyapatite-coated implant, Interface, Bonding

INTRODUCTION

Scientists have synthesized hydroxyapatite (HA), the mineral constituent of human hard tissues, by using various methods. Such products cannot be used alone for parts exposed to excessive stress, since they do not have bending strength and fracture toughness that are comparable to those of human hard tissues such as cortical bone. In order to overcome the insufficient mechanical properties and also to exploit its biocompatibility, HA has been used together with metal. HA-coated titanium or titanium alloy implant can accelerate bone formation that is required for the stabilization of implant; HA is expected to play the role of bioactive interface for the success of implant treatments.

Recently, electrochemical deposition of apatite has been investigated for surface modification of titanium[1−3]. However, plasma spraying is still a common method used to coat metal substrates with HA[4]. The process can start with depositions of HA, other calcium phosphates, and non-phosphates. The crystallinity of HA could be poor at those initial deposition areas[5,6]. The acid resistance of these compounds tends to be week, and the deposition layer may contain cracks that develop during the rapid cooling after spraying[7−9]. With these potential problems, we cannot underestimate the importance of the interface between coating and metal substrate for bond integrity. It is generally thought that the bond between coating and substrate is due to mechanical interlocking. On the other hand, the presence of Ca and P in the substrate seemed to suggest the presence of chemical bonding[7,8,10,11].

Little is known of the interface structure of HA-coated implants, while the crystal structure and composition of HA coating and its *in vivo* reaction and change have been investigated. The chemical stability and fracture resistance of the interface depends on its structure. In the present study, we aimed to morphologically and chemically characterize the interface between the coating and substrate of a commercially available dental implant coated with plasma-sprayed HA, by means of electron probe microanalysis (EPMA) and X-ray photoelectron spectroscopy (XPS).

MATERIALS AND METHODS

The experimental specimen was a Ti-6Al-4V implant, Integral® Calcitek® (Lot No. 983916, SULZER medica, Carlsbad, CA). The cylinder-type implant, 4 mm in diameter and 15 mm in length, had a round apex design and a plasma-sprayed HA-coating layer of approximately 50 μm thickness. Implants were randomly selected for various analyses.

Element distribution at coating-substrate interface

Using an electron probe microanalyzer (EPMA-8705 H-II, Shimadzu, Kyoto, Japan), element distributions at the coating-substrate interface were analyzed on samples prepared by three methods given below.

(1) To dissolve the coating material, one implant was immersed in 1N HCl solution for 1 hour and ultrasonically cleaned. The exposed surface was sputter-coated with gold and analyzed for Al, Ca, P, and O in a sample-scanning mode of 1 μm/step. Since Ca and P contents were expected to be very low, these elements were analyzed under high-sensitive analysis conditions: a high sample current of 0.5 μA and a long sampling time of 800 ms/step.

(2) Using a diamond wheel (11-305, RefineTech, Yokohama, Japan) and silicone cutting oil (Special-Oil-VP 3099, Fritsch, Hagen, Germany) at 200 rpm on a cutting machine (Minicut 40, Fritsch, Hagen, Germany), implants were transversally cut into circular disks approximately 2-mm thick. Two disk samples from different implants were diametrally loaded at a crosshead speed of 0.1 mm/min on a universal testing machine (Autograph AG-1000E, Shimadzu, Kyoto, Japan) until partial exfoliation of the coating took place near the loading platens (Fig. 1). The exposed substrate surface was ultrasonically cleaned, coated with evaporated carbon film, and analyzed for Ti, Al, Ca, and P under normal analyzing conditions. After this analysis the fragmented coating material that remained on the substrate surface was exposed to the HCl solution as described above and then coated with carbon film. The same area as previously investigated was re-analyzed for Ti, Ca, P, and C. The high-sensitive analysis conditions were again adopted for Ca and P. The above sequence was repeated for the second sample to check for experiment reproducibility.

(3) Similarly, four disk samples were prepared from different implants. After the side wall of each disk was masked with adhesive tape, the disk was hammered at the center to exfoliate the coating. The substrate-side surface of the material which adhered to the tape was sputter-coated with gold and analyzed for Ca, P, O, and C under normal analyzing conditions.

Diffusion of Ca and P into metal substrate

One disk sample was embedded in acrylic resin in such a way that the longitudinal axis of the implant was inclined at approximately 10° to the horizontal plane. The sample was wet-ground with waterproof abrasive papers, polished with a diamond paste (Diapaste 6 μm, Kasai, Tokyo, Japan), ultrasonically cleaned, and finally carbon-coated. Distributions of Ca and P in the substrate were analyzed in the vicinity close to the substrate-coating boundary by the beam-scanning mode of EPMA.

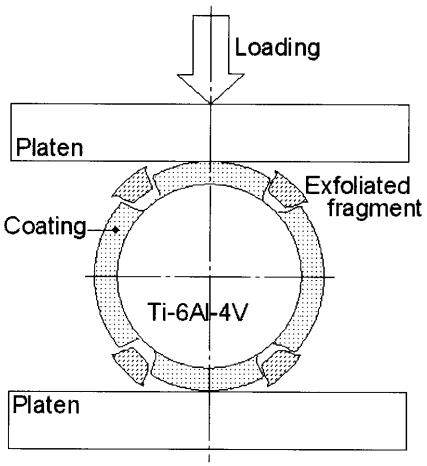

Fig. 1 Diametral loading of transversally cut disk of implant. HA-coating was exfoliated symmetrically at four points near the loading platens.

Chemical bond states of Ti, Ca, C, and P in substrate surface

Two implant samples were immersed in the HCl solution described above, and thereby the metal surface was exposed. To investigate the chemical bond states of Ti, Ca, C, and P in the substrate surface, an area of 6 mm in diameter — from each implant sample — was analyzed in a vacuum of 1 μPa on an X-ray photoelectron spectrometer (JPS-71XPS1, JEOL, Tokyo, Japan) using MgK α generated at 10 kV and 20 mA. At a step width of 0.1 eV, the binding energy ranges were scanned at a sampling time of 0.5 s/step for Ti *2p* and C *1s*, and that of 2.5 s/step for Ca *2p* and P *2p*. Depth profiling was attempted by repeating the combination of Ar sputtering and XPS analysis. The sputtering rate was 0.6 nm/s for silica as reference. Peak shifts of these elements were compared with standard data available in published literature[12–14].

RESULTS

Element distribution at coating-substrate interface

The sample treated with HCl exhibited rough substrate surface (Fig. 2(a)). While the surface showed overall low O content, it also contained areas of high O content (Fig. 2(b)). The former was evidently due to the presence of titanium oxides at the substrate surface. The latter indicated that the substrate alloy had been roughened by Al_2O_3 grit blasting prior to HA spraying, as Al also coexisted in these areas (not shown). The substrate surface also showed overall low Ca and P distributions, except for the locations where Al_2O_3 particles remained (Figs. 2(c), (d)). No exact correlation was found between the Ca and P maps. This might be partly caused by surface unevenness: the directions normal to the depression slopes were different from point to point with respect

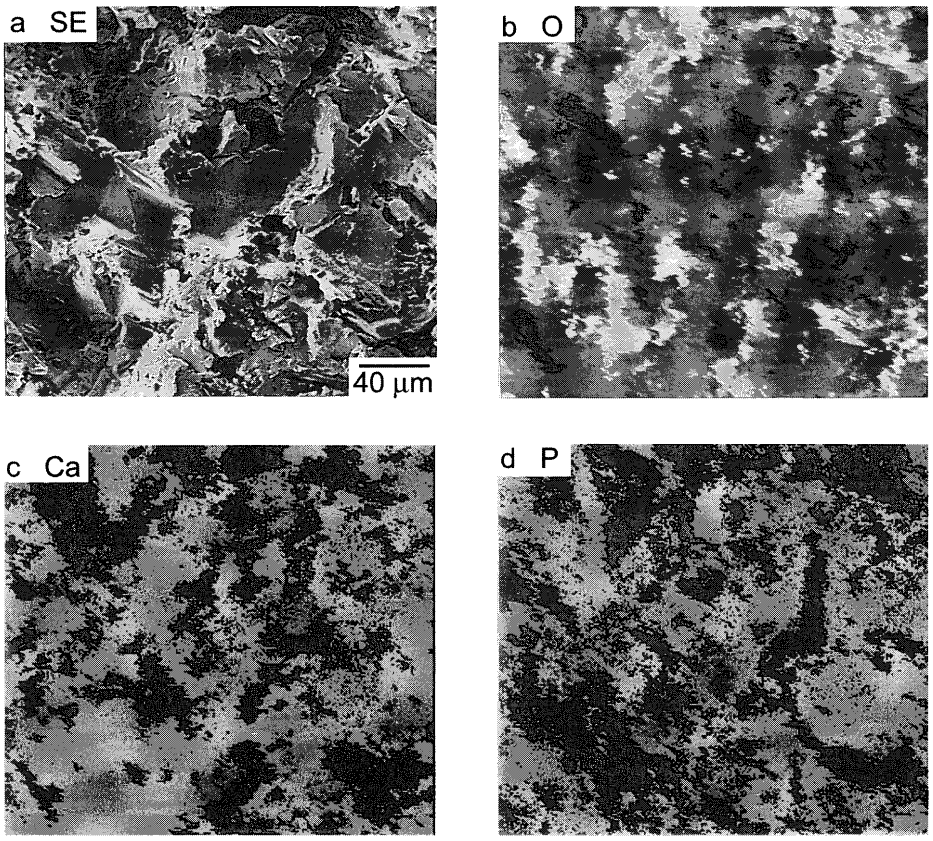

Fig. 2 Results of EPMA conducted on substrate surface exposed by HCl-dissolution of HA-coating. The element distribution maps are displayed with respective five-level gray scales.

to the location of each element detector.

Fig. 3(a) shows the substrate surface that was mechanically exposed by diametral compression. The surface was characterized by differences in Al content: little, low, or high (Fig. 3(c)). Mapping of Ti (Fig. 3(b)) confirmed that the low Al content areas represented the substrate alloy and the high Al content areas were the embedded Al_2O_3 particles. The distributions of Ca (Fig. 3(d)) and P (not shown) were in reverse proportion to that of Ti, indicating the presence of remaining coating fragments. The mechanically exposed surface appeared relatively even in comparison with the chemically exposed surface (Fig. 2(a)), as concavities present on the substrate surface were filled with remaining coating fragments. This was confirmed as the surface irregularities became more distinct after the sample received additional acid treatment (Fig. 3(e)). The acid treatment also revealed that Ca (Fig. 3(f)), though in very low content, was detected in the previously exfoliated areas rather than in the areas where remaining coating fragments were found. A similar finding was confirmed in P (Fig. 3(g)). Again, no distinct correlation was found between the maps of Ca and P. Carbon was unevenly distributed throughout the substrate surface, and its contents were very high in the previously exfoliated areas (Fig. 3(h)).

Fig. 4(a) shows the coating that adhered to the masking tape. Apart from heavy cracking due to the hammering, the observed surface was relatively even, again indicating that fragments of coating material were held in concavities present on the substrate surface.

The oval-shape halation shown at the top of Fig. 4(a) demonstrates high Ca, P, and O contents (P and O maps not shown). It was found that similar round particles were formed in the area, which had been subjected to element analysis (Fig. 5).

Unexpectedly, Ca-deficient areas were found (Fig. 4(b)). Similar observations were confirmed for P and O (not shown). These Ca-, P-, and O-deficient areas were very rich in C (Fig. 4(c)). However, high concentration of C was not found in the exterior surface of the coating.

These results were confirmed by three other samples analyzed.

Diffusion of Ca and P into metal substrate

Fig. 6(a) shows an SE image of the vicinity close to the boundary between coating and metal substrate.

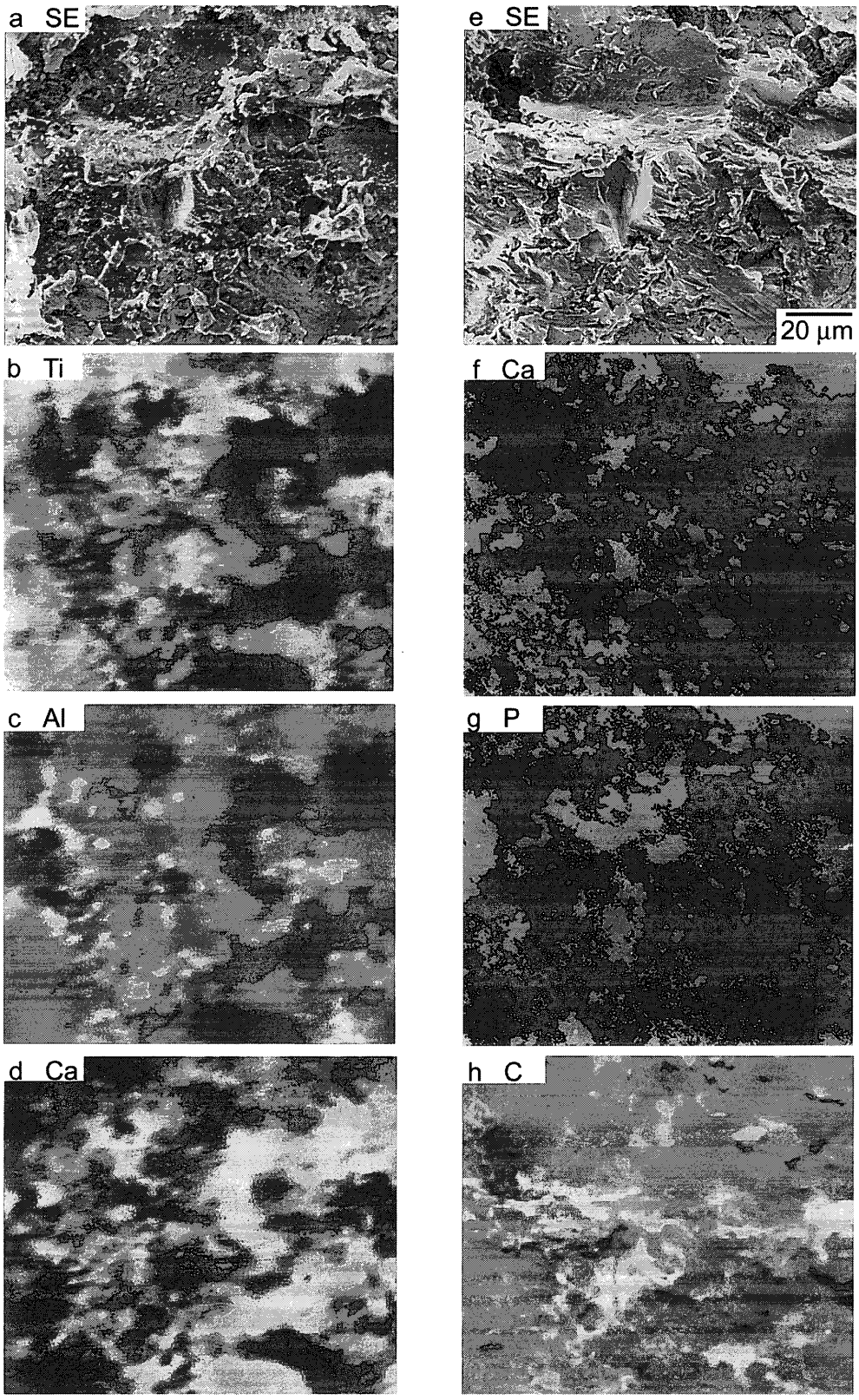

Fig. 3 Results of EPMA conducted on substrate surface.
(a)-(d) Surface exposed by diametral loading.
(e)-(g) Re-analysis of the same area after additional treatment with HCl solution. The element distribution maps are displayed with respective five-level gray scales.

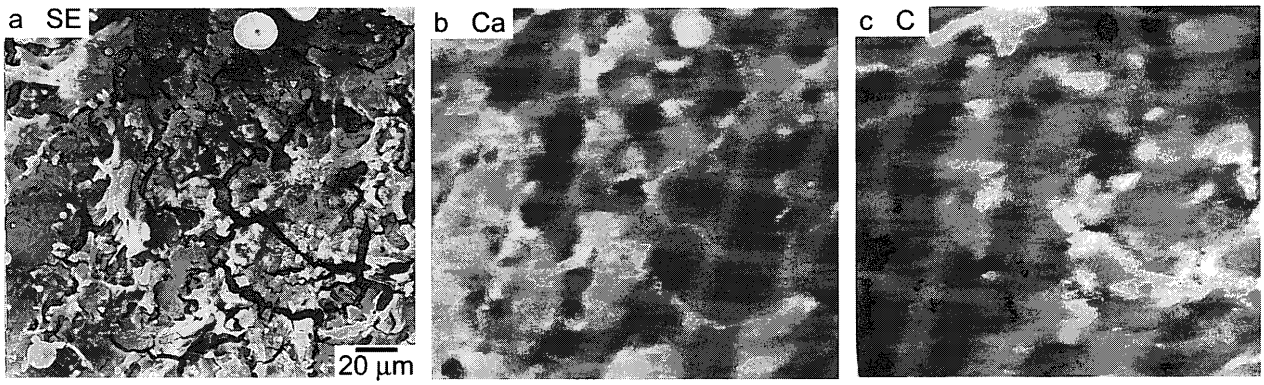

Fig. 4 Results of EPMA conducted on substrate-side surface of HA-coating fragment. The fragment was obtained by hammering the implant disk at the center. The element distribution maps are displayed with respective five-level gray scales.

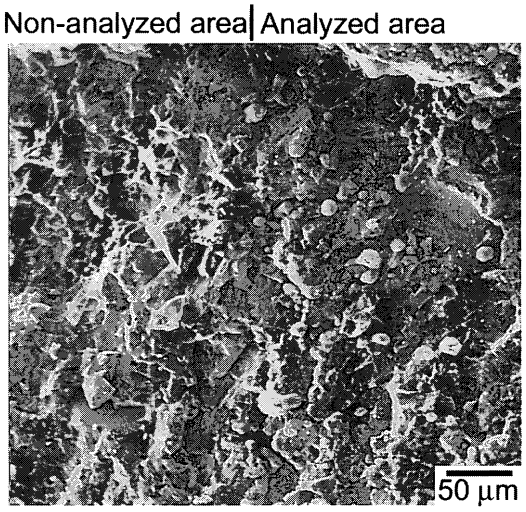

Fig. 5 Morphological change of substrate-side surface of HA-coating during EPMA. SE images before and after EPMA are shown on left and right sides, respectively.

The latter is identified by abrasive-induced scratches and Al_2O_3 particles are observed as dark spots. For representative demonstration of Ca and P distributions around the boundary, averaged CaKα and PKα intensities in the area between the two parallel lines are shown as line profiles in Fig. 6(b). The Ca content decreased gradually from the boundary within a depth of up to 5 to 10 μm, while the P content decreased rapidly to the background level at the boundary. The difference indicated a higher diffusion of Ca than P into the metal substrate.

Chemical bond states of Ti, Ca, C, and P at substrate surface

Fig. 7 shows the XPS analysis results. Peaks of Ti *2p3/2* were assigned to TiO_2 and then metallic Ti, as the analysis shifted deeper into the substrate. The oxide film was of nanometer order in thickness. In one sample, weak peaks of Ca *2p3/2* and P *2p* were found at the outermost surface (Figs. 7(b), (d)). In another sample, only P *2p* peak was found (not shown). Comparison of the Ca *2p*, P *2p*, and Ti *2p* depth profiles suggested the presence of Ca and P in the oxide film. The XPS analysis did not detect any metallic Ca diffused into the metal substrate, probably due to its low content. C *1s* peaks first appeared at higher energies and then at a lower energy (Fig. 7(c)). The latter peak might be assigned to TiC.

DISCUSSION

Element distribution at coating-substrate interface

When a disk is diametrally loaded, low tensile stress tangential to the circumference is induced near the loading points[16], which could cause local exfoliation of the coating layer (Fig. 1). The partial exfoliation of coating layer at these points exhibited a macroscopically cohesive fracture, but the elemental analysis of the surface indicated a mixed mode of interfacial and cohesive fractures at microscopic level (Figs. 3(b), (d)). After the subsequent HCl treatment, low levels of Ca and P were still present at the interfacial fracture surface (Figs. 3(f), (g)) where Ti was previously exposed (Fig. 3(b)). This observation was different from that obtained with the substrate that received HCl-immersion alone, as this treatment left Ca and P all over the substrate surface except for locations where Al_2O_3 particles were detected (Fig. 2). Moreover, the XPS analysis indicated that Ca and P were present mainly in the oxide film on the substrate (Fig. 7).

A number of round particles with high contents of Ca, P, and O were observed on the substrate-side surface of coating that had been subjected to element analysis (Figs. 4 and 5). During element analysis, temperature of the sample with lower heat conductivity was raised more substantially. Therefore, calcium phosphates with low melting points melted due to the heat and then solidified subsequently. It is

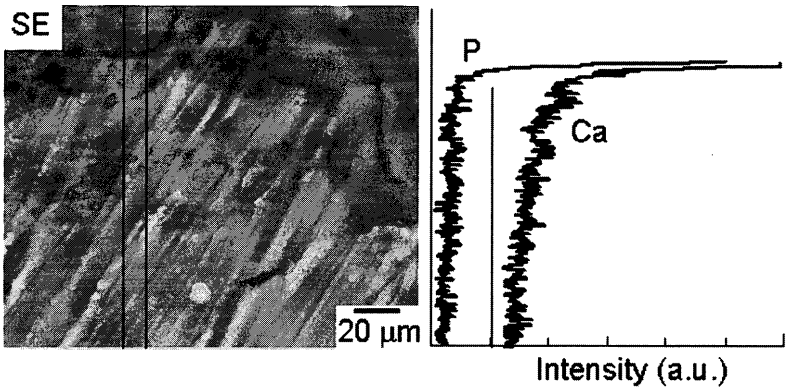

Fig. 6 Ca and P distributions from HA-coating to substrate. Line profiles of CaKα and PKα intensity are shown as average in area between parallel lines.

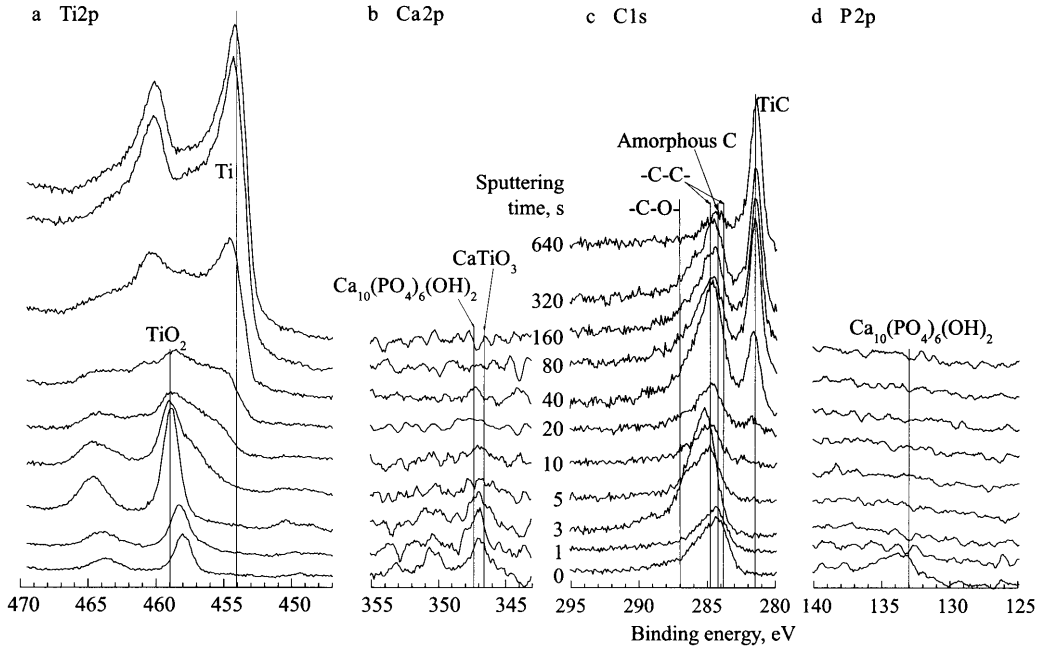

Fig. 7 Results of XPS conducted on substrate surface immersed in HCl solution: Ti (a), Ca (b), C (c), and P (d).

known that plasma spraying induces partial changes of HA into non-apatite phases such as amorphous phosphates, TTCP, and TCP[10,15]. The coating near the interface is believed to be rich in amorphous phases and calcium phosphates other than HA[5,6]. Since TTCP and TCP have relatively high melting points, the round particles on the analyzed surface might have included other calcium phosphates or amorphous phases.

Diffusion of Ca and P into metal substrate

Ducheyne *et al.*[10] sintered electrophoresed HA on a Ti plate and analyzed the section perpendicular to the interface by energy dispersive spectroscopy (EDS). They concluded that preferential diffusion of P occurred. Filiaggi *et al.*[7] prepared an ultra thin film from a HA-plasma-sprayed Ti-6Al-4V alloy implant. Their electron energy loss spectroscopy (EELS) results on the film showed that the diffusion of P into the substrate was in the order of 20-30 nm. There were no indications of Ca diffusion. In contrast, Brantley *et al.*[11] and Tufekci *et al.*[8] in their EDS studies reported the preferential diffusion of Ca.

The above discrepancy could be attributed to three factors. Firstly, methods employed in sample preparation were different between investigators. The interface layer (3-6 μm) obtained by Ducheyne *et al.*[10] was very thick as compared with that formed by HA spraying. Secondly, these analyses might not provide data precise enough to discuss diffusion.

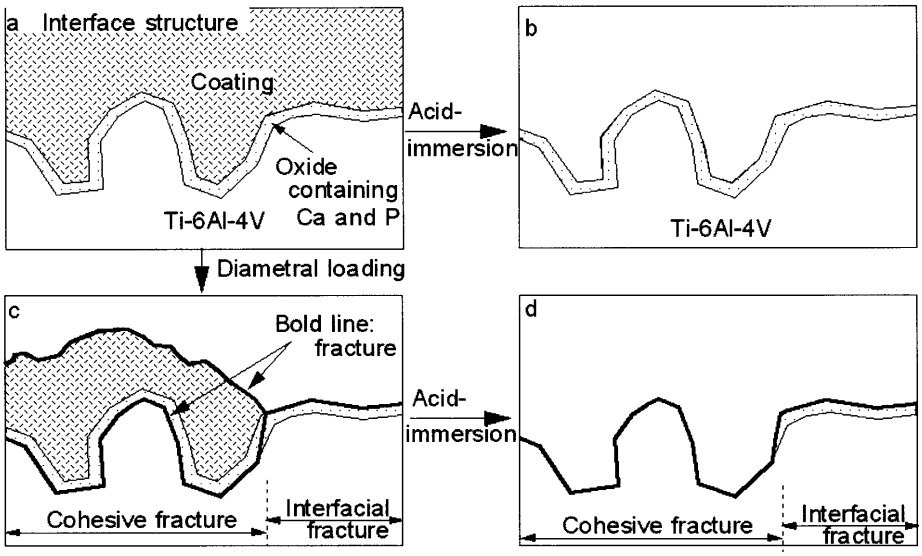

Fig. 8 Postulated interface structure model and fracture mode. The thickness of oxide film is exaggerated. Alumina particles are omitted here.

Space resolution generally attainable is comparable to the expected diffusion distance, while a very fine space resolution available with EELS can accidentally analyze a non-representative area, as the investigators pointed out[7]. Finally, the obtained results were discussed in terms of the difference in ionic sizes between Ca and P. While ionic radius is of significance in the case of oxides, it has no physical bearing in the case of alloys. Thus, in the present study the plane to be analyzed was inclined by 10° in consideration of the space resolution of EPMA. In this way, the apparent distance was extended approximately 5 times above the original distance. The accelerating voltage was reduced from 20 kV to 15 kV so as not to capture any X-ray signal from the underlying coating, and the position to be analyzed was clearly defined. This method has given an estimation that the metallic diffusion of Ca beyond the oxide film was within a few μm of the substrate (Fig. 6). The diffusion could have taken place during the heat treatment after spraying, which was intended to improve HA crystallinity and coating-alloy bond.

Nakajima *et al.*[17] reviewed widely the diffusibility of various elements in Ti, and demonstrated that elements with low solubility in Ti can diffuse faster than those with high solubility. For example, the diffusion coefficient of P is four to five orders higher at 1100 K, compared to that of Ti self-diffusion. The solubility of P in α-Ti is ~0.3 at%, whereas that of Ca is ~0.05 at%[18]. Although the data of Ca diffusion are not found in the review, the difference in solubilities between P and Ca may account for the present results. However, the possibility of P diffusion is not entirely discarded, because the analyzed lines were restricted within several numbers.

Microstructure and fracture model at interface

Based on the present results, it is possible to postulate an interfacial fracture model for HA-coated Ti or Ti alloy implants (Fig. 8). A thin titanium oxide film containing Ca and P was present at the interface (Figs. 8(a), (b)), as Ca and P in low contents were widely detected in the substrate surface exposed by the simple HCl treatment (Figs. 2(c), (d)). This was further confirmed in the comparison made between the depth profile of Ti *2p* with those of Ca *2p* and P *2p* (Figs. 7(a), (b), and (d)).

Diametral loading exfoliated the coating from this film at places where the bond was weak (interfacial fracture on the right side of Fig. 8(c)). Since the oxide film remained attached to the substrate (right side of Fig. 8(d)), Ca and P in low contents could be detected in the interfacial fracture area (Figs. 3(b), (f), and (g)). On the other hand, at places where the coating was strongly bonded to the oxide film, the loading exfoliated the coating together with the film from the underlying substrate (cohesive fracture on the left side of Fig. 8(c)). Simultaneously, the coating fractured cohesively into fragments but many fragments remained mechanically held in concavities present in the substrate. During the HCl treatment after loading, the oxide film which was attached to the exfoliated fragments, while highly acid-resistant, was lost along with the dissolution of the fragments (left side of Fig. 8(d)). Ca and P were thus hardly detected in the substrate beneath the remaining fragments (Figs. 3(d), (f), and (g)).

The observed Ca diffusion into the metallic substrate indicated the continuity between coating and substrate, implying chemical bond[7,8,10,11]. The present

results indicated, however, that the fractures at both the interfaces between the coating and oxide film and between the alloy and oxide film occurred as interfacial and cohesive fractures, respectively. In other words, the mechanical interlocking action due to surface irregularities is still the major factor which determines bond integrity.

C and its influence on coating-substrate bond

High C content areas were present in the interior (substrate-side) surface of coating fragment (Fig. 4) but not on the exterior surface. Carbon also concentrated in the interfacial fracture areas on the substrate of the diametrally-loaded specimen (Figs. 3(b), (h)). However, it was difficult to identify the C-rich phase by EPMA. Moreover, C was widely distributed in the depth direction (Fig. 7(c)). The TiC-like phase might be formed by reaction between substrate and C during spraying. Since the details of plasma-spraying technique are proprietary to manufacturer, it is unknown whether the incorporation of C is intentional or not. It may be assumed that the carbon originated from hydrocarbons which had been present on the substrate before spraying. However, this hypothesis alone fails to account for the high C content indicated by EPMA. Further investigation is therefore needed to understand the influence of C on the bond strength between coating and substrate.

CONCLUSION

In the present study, an attempt was made to morphologically and chemically characterize the interface between the coating and substrate of a commercially available plasma-sprayed HA-coated implant. A thin titanium oxide film containing Ca and P was found at the interface. When the implant was subjected to mechanical stress, a mixed mode of cohesive and interfacial fractures occurred. The cohesive fracture was due to separation of the oxide film from the substrate, while the interfacial fracture was due to exfoliation of the coating from the oxide film bonded to the substrate. The diffusion of metallic Ca into the metal substrate implied the presence of chemical bond at the interface. However, mechanical interlocking appeared to play the major role in HA-coated Ti and Ti alloy implants, as many coating fragments remained in concavities present on the substrate surface.

REFERENCES

1) Ban S, Matsuo K, Mizutani N, Hasegawa J. Hydrothermal-electrochemical deposition of calcium phosphates on various metals. Dent Mater J 1999; 18: 259-270.
2) Ban S, Kamiya A, Sonoda T. Calcium-ion incorporation into titanium surfaces accompanied by electrochemical apatite-deposition. Dent Mater J 2002; 21: 306-313.
3) Ban S. Real-time monitoring of apatite deposition using electrochemical quartz crystal microbalance. Dent Mater J 2003; 22: 467-474.
4) de Groot K, Geesink R, Klein CPAT, Serekian P. Plasma sprayed coatings of hydroxyapatite. J Biomed Mater Res 1987; 21: 1375-1381.
5) Gross KA, Berndt CC, Herman H. Amorphous phase formation in plasma-sprayed hydroxyapatite coatings. J Biomed Mater Res 1998; 39: 407-414.
6) Baltag I, Watanabe K, Kusakari H, Taguchi N, Miyakawa O, Kobayashi M, Ito N. Long-term changes of hydroxyapatite-coated dental implants. J Biomed Mater Res (Appl Biomater) 2000; 53: 76-85.
7) Filiaggi M, Coombs NA, Pilliar RM. Characterization of the interface in the plasma-sprayed HA coating/Ti-6Al-4V implant system. J Biomed Mater Res 1991; 25: 1211-1229.
8) Tufekci E, Brantley WA, Mitchell JC, Mcglumphy EA. Microstructures of plasma-sprayed hydroxyapatite-coated Ti-6Al-4V dental implants. Int J Oral Maxillofac Implants 1997; 12: 25-31.
9) Lacefield WR. Characterization of hydroxylapatite coatings. J Oral Implantology 1994; 20: 214-220.
10) Ducheyne P, Raemdonck W, Heughebaert JC, Heughebaert M. Structural analysis of hydroxyapatite coatings on titanium. Biomater 1986; 7: 97-103.
11) Brantley WA, Tufekci E, Mitchell JC, Foreman DW, McGlumphy EA. Scanning electron microscopy studies of ceramic layers and interfacial regions for calcium phosphate-coated titanium dental implants. Cells and Mater 1995; 5: 73-82.
12) Ikeo N, Iijima Y, Niimura N, Shigematsu N, Tazawa T, Matsumoto S, Kojima K, Nagasawa Y. Handbook of X-ray photoelectron spectroscopy. JEOL, Tokyo, 1991; pp.157-211.
13) Briggs D, Seah MP. Practical surface analysis, 2nd ed., Vol. 1 Auger and X-ray photoelectron spectroscopy. John Wiley & Sons, Chichester, 1995; pp.607.
14) Asami K, Chen SC, Harazaki H, Hashimoto K. The surface characterization of titanium and titanium-nickel alloys in sulfuric acid. Corrosion Sci 1993; 35: 43-49.
15) Rey C. Calcium phosphate biomaterials and bone min eral—Differences in composition, structures and properties. Biomater 1990; 11: 13-15.
16) Ehrnford L. Stress distribution in diametral compression tests. Odontol Scand 1981; 39: 55-60.
17) Nakajima H, Koiwa M. Diffusion in titanium. Bull Jpn Inst Metals 1991; 30: 526-535.
18) Murray JL (editor). Phase diagrams of binary titanium alloys. ASM International, Ohio, 1987; pp. 52-53 and pp.234-235.